Jurnal Penelitian Fisika dan Aplikasinya (JPFA)
Volume 12, Issue 2, December 2022
https://journal.unesa.ac.id/index.php/jpfa/

p-ISSN: 2087-9946
e-ISSN: 2477-1775

Impact of Ti^{4+} Substitution on Structure and Conductivity of $LiNi_{0.8}Mn_{0.1}Co_{(0.1-x)}Ti_xO_2$ as Battery Cathode (x = 0.01, 0.02, and 0.03)

Maya Puspitasari Izaak [1,a], Yohanes Edi Gunanto [1,b,*], Henni Sitompul [1,c], and Yustinus Purwamargapratala [2,d]

[1] Department of Physics Education, Faculty of Education, Pelita Harapan University, Karawaci, Tangerang 15811, Indonesia
[2] Center for Science and Technology of Advanced Materials, BRIN, Tangerang Selatan 15314, Indonesia

e-mail: [a] maya.izaak@uph.edu, [b] yohanes.gunanto@uph.edu, [c] henni.sitompul@uph.edu and [d] pratala_yustinus@yahoo.com
* Corresponding Author

Received: 20 June 2022; Revised: 19 Agustus 2022; Accepted: 17 September 2022

Abstract

Various cathodes have been studied to obtain cathode materials with high energy density and are inexpensive and environmentally friendly. Ti^{4+} substitution is one strategy to achieve this. Ti^{4+} doping has been done on Co^{2+} to reduce the level of toxicity. The objective of this research was to look at the impact of Ti^{4+} substitution on $LiNi_{0.8}Mn_{0.1}Co_{(0.1-x)}Ti_xO_2$ so that it can be used as a battery cathode. The samples were prepared by the solid-state reaction method using high energy milling (HEM) in a wet state using ethanol. The phase formation of the material was characterized using XRD, surface morphology was characterized using SEM, and electrical conductivity was characterized using LCR-Meter. The finding showed that the particles experienced agglomeration, with the average size of the primary particles ranging from 300-500 nm and the secondary particle sizes ranging from 1-3 μm. The morphology of the sample shows polycrystals. The maximum electronic conductivity obtained was 2.3 x 10^{-5}, 2.4 x 10^{-5}, and 3.2 x 10^{-5} S/cm for x = 0.01, 0.02, and 0.03, respectively. Another impact is increasing the cell volume and conductivity. With this high electrical conductivity value, this material is suitable for use as a battery cathode.

Keywords: *Ti doping; cathode; battery*

How to cite: Izaak M P, et al. Impact of Ti^{4+} Substitution on Structure and Conductivity of $LiNi_{0.8}Mn_{0.1}Co_{(0.1-x)}Ti_xO_2$ as Battery Cathode (x = 0.01, 0.02, and 0.03). *Jurnal Penelitian Fisika dan Aplikasinya (JPFA)*. 2022; **12**(2): 92-101.

INTRODUCTION

The growing awareness of environmental issues and the scarcity of fossil fuels have necessitated the development of alternative propulsion energy sources in recent decades. For example, the regular operation of battery electric vehicles (BEVs) produces zero exhaust emissions [1]. Conventional lead-acid batteries have been replaced by lithium-ion batteries (LIBs) within the energy production sector. The emergence of large-scale devices, such as electric cars

DOI: 10.26740/jpfa.v12n2.p92-101

(EVs) and energy storage systems (ESSs), has significantly increased the demand for LIBs [2].

Among all battery components, the cathode continues to be a critical limiting factor for energy density and power improvements. [3]. Cathode materials in LIBs must be capable of reversibly intercalating Li-ions without substantial changes to the atomic structure. In this instance, lithium metal oxides, LiMO2, are commonly used cathode materials, where M is a pure metal or a transition metal combination such as nickel (Ni), cobalt (Co), titanium (Ti), iron (Fe), and manganese (Mn) [4].

Research has been done on a variety of cathodes with the goal of increasing the energy density of LIBs to fulfill the requirements. Among cathode materials, the Ni-rich NCM811 cathode has been extensively studied for high-energy LIBs because of its relatively low cost, environmental factors, and increased specific capacity [2]. However, Ni-rich (Ni 80%) NCM cathodes have several issues, including insufficient cycle life and diminishing capacity, which limit commercialization. [5,6]. Therefore, a comprehensive risk assessment of their safety is urgently needed. It has been proven established that the thermal stability of NMC reduces as the Ni concentration increases, corresponding to an increase in capacity and a reduction in material costs [7]. Researchers have tried anion/cation doping to alter the formulation, concentration gradient structure, core-shell, and surface coating, for example, by changing the surface with conductive materials like TiO_2 [8].

The integration of foreign ions, including cations and anions, is one of the simplest and most prevalent methods for enhancing Ni-rich layered oxides' structural and thermal stability. Further, both Li and transition metal sites are taken into account for cation doping. The Li site may also contain various alkali metals at the Li site. Ions with no electrochemical activity, such as Na^+ [9] and Ti^{4+} or other cation dopants, are proposed to prevent cation mixing, reduce oxygen release, and strengthen structural stability [10]. The partial substitution of transition metals is another method for enhancing material characteristics. Co is emphasized because of its high toxicity and cost, while Mn is disregarded because of its electrochemical passivity. [11].

Generally, adding the Ni concentration increases the capacity and decreases the expense, but it decreases the structural and thermal stability. However, significant obstacles exist, such as the low ionic conductivity of solid electrolytes and the destabilization of the interface [12]. Research findings show that replacing Ti^{4+} with other ions can stabilize the electrolyte and enhance the performance of cathodes [13,14], but make the ionic conductivity decrease [15]. However, there are ongoing debates around the issues with the NMC811 cathode material. We use a composition with a significant nickel content and Ti^{4+} substitution in Co^{2+} to reduce the toxic nature of cobalt. Previous studies have never studied this composition as a cathode material. This study looks at how adding Ti^{4+} ions to Co^{2+} ions affects the crystal structure, surface shape, and electrical conductivity of $LiNi_{0.8}Mn_{0.1}Co_{0.1-x}Ti_xO_2$ compounds with x = 0.01, 0.02, and 0.03.

METHOD

The raw materials Li_2O (Merck), NiO (Merck), $MnCO_3$ (Merck), Co (Merck), and TiO_2 (Merck), each with a purity above 99% was weighed according to stoichiometric calculations to form the compound $LiNi_{0.8}Mn_{0.1}Co_{(0.1-x)}Ti_xO_2$ (x = 0.01, 0.02, and 0.03). Equation (1) is the reaction equation used.

$$Li_2O + NiO + MnCO_3 + Co + TiO_2 \rightarrow LiNi_{0.8}Mn_{0.1}Co_{(0.1-x)}Ti_xO_2 + CO_2 \quad (1)$$

Each of these raw materials was put into a stainless-steel vial and equipped with stainless

steel balls with a ratio of 1:1 for the weight of the material and iron balls. Then the mixture was milled in a wet state using alcohol for 30 hours, with stages every 60 minutes of milling interspersed with 30 minutes of rest. The samples were then dried in an oven at 80°C. In phase formation, the sample was sintered at 1000°C and held for 5 hours in the air. The temperature then returned to room temperature. The phase formation was characterized using Cu-K radiation with a wavelength of 1.5406 at a diffraction angle of 2θ = 20° - 80°, utilizing an X-ray diffractometer (XRD) of Philips PW1710 type. We use continuous measurements with a step size of 0.263°, so there is no dwell time. We choose 2θ = 20° - 80° because, according to the literature, the first peak appeared at an angle of 2θ less than 20° but more than 10° [16-18]. To see the surface morphology, scanning electron microscopy (SEM) type-JEOL, JED 2300 was used, and LCR meter type HIOKI 5020 was utilized to measure the electrical conductivity at room temperature.

RESULTS AND DISCUSSION

Figure 1 shows the diffraction patterns of X-ray diffractometer results. The Rietveld program characterization results showed that all samples were in phase because the second phase was not detected. So, it can be said that the Ti^{4+} ion succeeded in substituting the position of the Co^{2+} ion. According to H. Sun et al., with the subsequent high-temperature solid-state reaction, Ti diffuses into NCM811 crystals and is uniformly distributed throughout the bulk of secondary particles [19]. All samples have a rhombohedral crystalline structure with space group R-3mH. In comparison, the same results were obtained by J. D. Steiner et al. [5].

Table 1 presents the complete XRD characterization data. There was a decrease in cell mass and density with increasing the Ti^{4+} doping. On the other hand, the volume increased with increasing the Ti^{4+} values. This is supported by the results of D. Y. Wan et al. [20]. The increase in cell volume can be explained by the fact that the ionic radius of Ti^{4+} (1.025 Å) is larger than that of Co^{2+} (0.885 Å). The diffraction pattern peaks can be indexed with ICDD card No. 01.078.7219. The peaks correspond to references at angles of 2θ= 18.8°, 38.3°, 44,406°, and 64,373° with Miller index (003), (102), (104), and (440), respectively.

Table 1. Rietveld refined result of $LiNi_{0.8}Mn_{0.1}Co_{(0.1-x)}Ti_xO_2$ with x = 0.01, 0.02, and 0.03, respectively

	x = 0.01	x = 0.02	x = 0.03
Space Group	R-3mH	R-3mH	R-3mH
Cell Mass	351.62(1)	345.80(1)	337.72(1)
Cell Volume (Å^3)	106.52(5)	106.70(1)	106.71(1)
Crystal Density (g/cm^3)	5.481(1)	5.382(1)	5.255(1)
Lattice Parameters: *a* (Å)	2.9305(2)	2.9320(2)	2.9323(1)
c (Å)	14.3226(1)	14.3315(3)	14.3311(2)
Rexp	2.36	2.39	2.42
Rwp	2.80	2.79	2.90
GoF	1.18	1.71	1.20

Crystal size is calculated using the Scherrer equation $D = k\lambda/(\beta \cos\theta)$, where k = form factor (0.89), λ= wavelength (Cu-kα = 1.5406 Å), β is the line broadening at half the maximum intensity (FWHM), and θ is the Bragg diffraction angle. From several dominant peaks, the

average crystal size ranged from 43.3 to 65.5 nm. This result is larger than the crystal size of NMC811 without the Ti doping obtained by H. Widiyandari et al., which is 45.37 – 46.74 nm [6]. This is following the XRD results; whereas the Ti value increases, the cell volume increases because the Ti^{4+} ion radius is larger than the Co^{2+} ion radius.

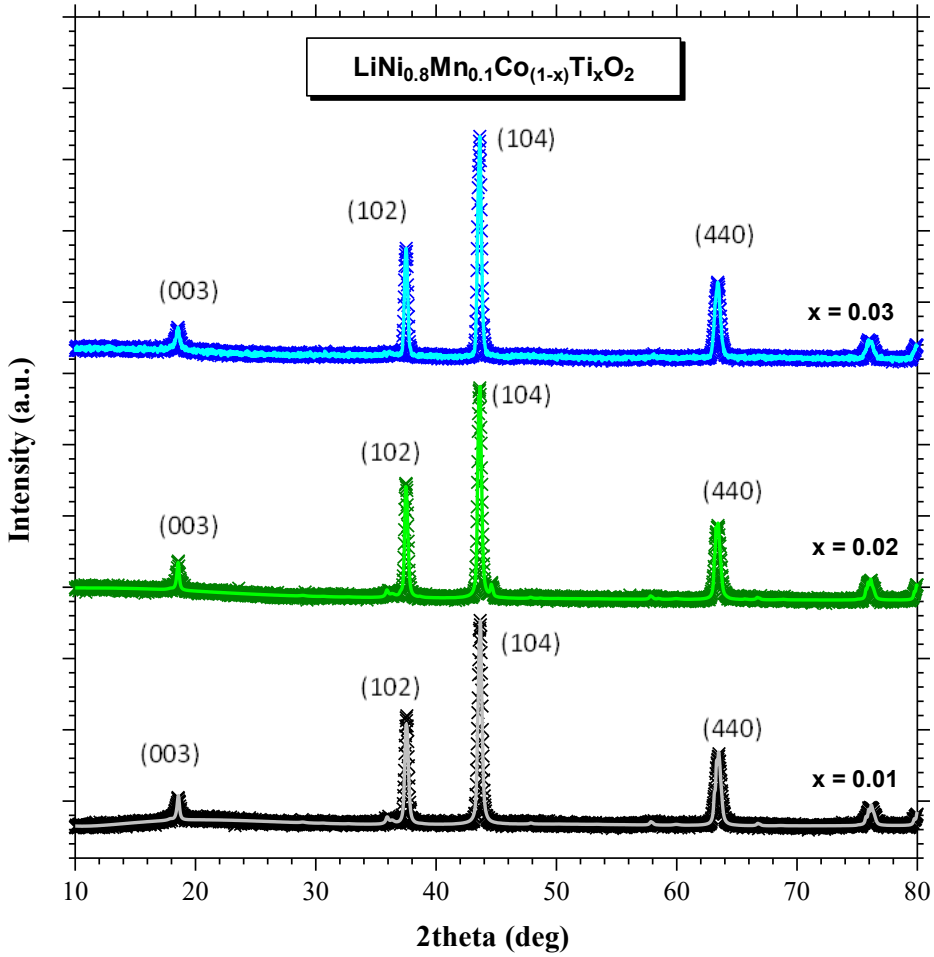

Figure 1. Rietveld refined powder XRD patterns of $LiNi_{0.8}Mn_{0.1}Co_{(0.1-x)}Ti_xO_2$ with x = 0.01, 0.02, and 0.03.

The surface morphology of the scanning electron microscopy (SEM) can be seen in Figure 2. The surface morphology of the sample has a heterogeneous grain shape and size. The particle size is obtained by comparing the grain length to the existing scale length.

The SEM findings indicate that the particles are aggregated. The average size of the primary particles ranges from 300-500 nm, and the secondary particle sizes range from 1–3 μm. Meanwhile, S.-J. Sim et al. obtained primary particle sizes ranging from 3-5 μm, and secondary particles ranging from 15-20 μm [2], D. Y. Wan et al. and H. Liu et al. produced primary particles between 200-500 nm, and secondary particle sizes of 3-5 μm [20, 21], while AA Savina obtained primary and secondary particle sizes of 100-500 nm and 0.8-1 μm, respectively [22]. The SEM results' morphology followed the XRD characterization results, where the sample showed polycrystals.

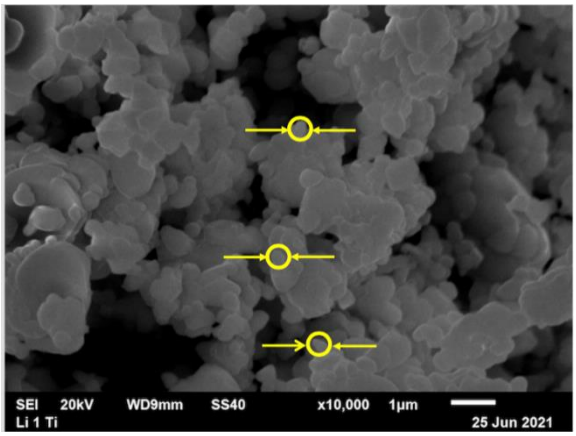

(a) Ti = 0.01

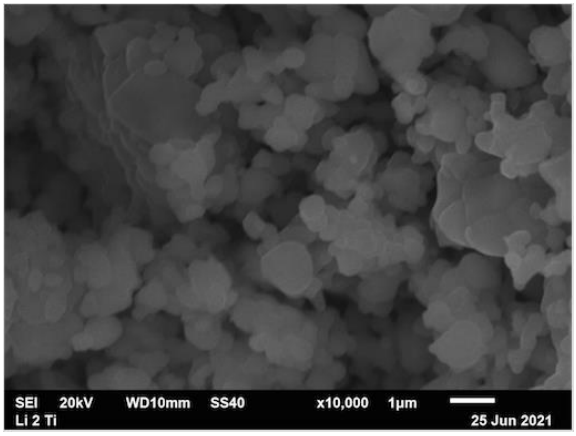

(b) Ti = 0.02

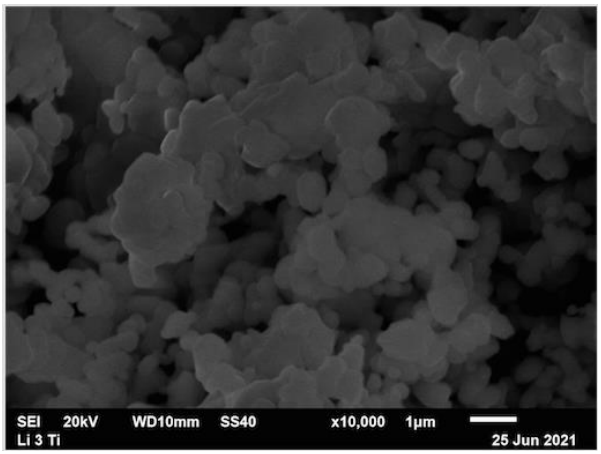

(c) Ti = 0.03

Figure 2. Surface morphology for Ti doping of samples $LiNi_{0.8}Mn_{0.1}Co_{(0.1-x)}Ti_xO_2$

Table 2. The value of mass (gram) of each raw material

	x = 0.01	x = 0.02	x = 0.03
Li_2O	3.8438	3.8481	3.8525
NiO	15.3736	15.3911	15.4087
$MnCO_3$	2.9574	2.9607	2.9641
Co	1.3645	1.2143	1.0637
TiO_2	0.2055	0.4114	0.6179

Table 2 describes the mass of each raw material required to form the $LiNi_{0.8}Mn_{0.1}Co_{(0.1-x)}Ti_xO_2$ sample with x= 0.01, 0.02, and 0.03. Surface morphology affects the cathode conductivity of high Ni-based Lithium Battery (LIB) cells [23, 24]. Large surface area can enhance power density and yield a greater specific capacity while providing susceptibility to electrolyte degeneration [25]. The high-power density results were also in high electronic conductivity [26]. Ti dopped can increase grain size. The increases in grain size also improved the conductivity as obtained by Dao Yong Wan et al. [27].

The electrical conductivity in a log scale that depends on frequency can be observed in Figure 3, and the graph of composition dependence of the electrical conductivity can be seen in Figure 4. The maximum electronic conductivity obtained is 2.3×10^{-5}, 2.4×10^{-5}, and 3.2×10^{-5} S/cm for x = 0.01, 0.02, and 0.03, respectively. This result is better than NMC811 without Ti

doping, which is 2.8 x 10^{-5} S/cm, even higher than the electrical conductivity of NMC111 (5.2 x 10^{-8} S/cm) [28]. Thus, Ti^{4+} substitution can increase the conductivity so that this material can be used as a battery cathode. Also, Ti^{4+} ion-doped can improve cyclic stability by increasing the distance between layers [29] and stabilizing the electrolyte [30]. Also from Figure 3, the substitution of Ti, in addition to increasing conductivity, can reduce the use of cobalt, which is toxic, making it safer for the environment [31-33].

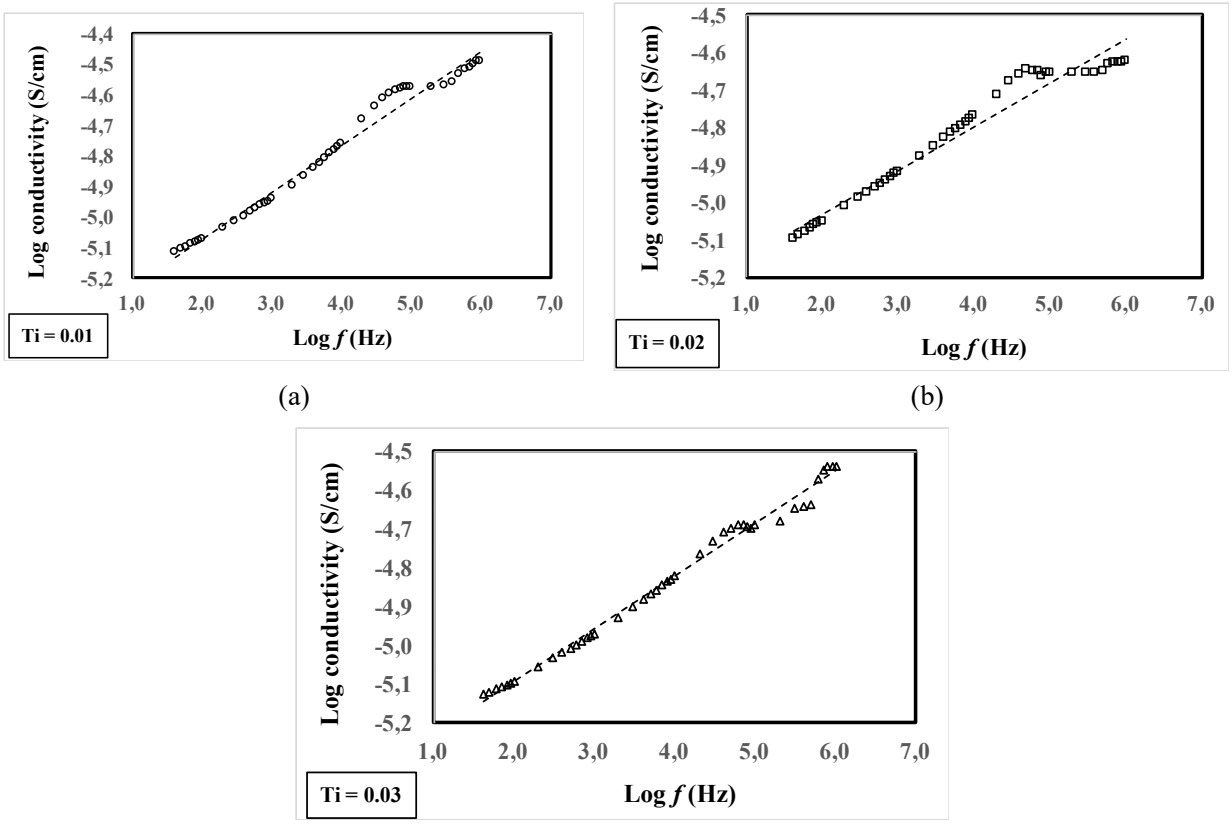

Figure 3. The frequency-dependent conductivity of the sample $LiNi_{0.8}Mn_{0.1}Co_{(0.1-x)}Ti_xO_2$ (a) x = 0.01, (b) x = 0.02, and (c) x = 0.03

The weakness of this study is that we have not arrived at a characterizing battery cycle life to measure the charge/discharge of this composition. Battery cycle life is the number of charges and discharge cycles a battery can complete before it loses performance. The cycle life of lithium-ion batteries is greatly affected by the depth of discharge, in which the discharge depth is the battery's total storage capacity [34].

This research is a form of support for the Indonesian government's project in downstream nickel mining products. Due to the abundant availability of nickel, Indonesia can become the producer of electric batteries, where nickel can be utilized from upstream to downstream. The prospects for nickel in the global market are bright as the electric vehicle (EV) industry continues to grow.

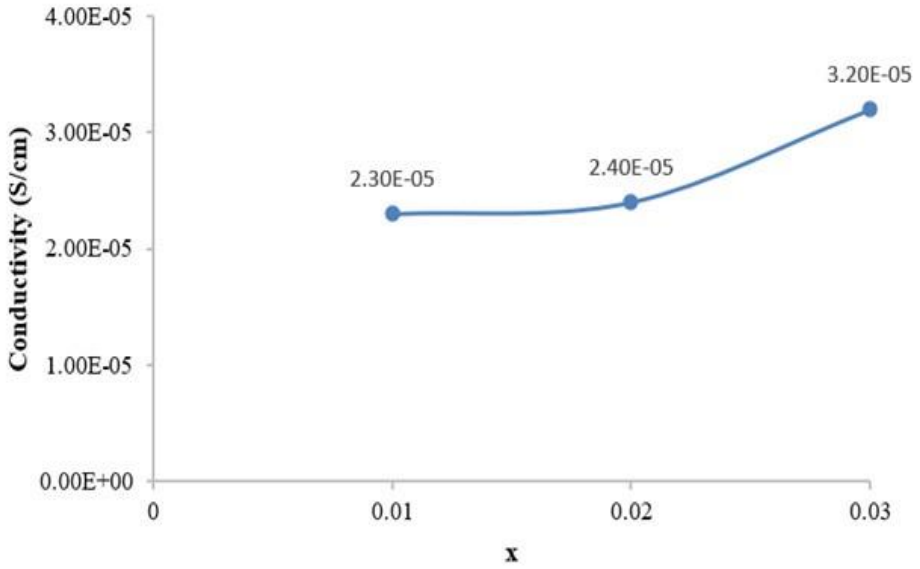

Figure 4. The composition dependence of conductivity of the sample $LiNi_{0.8}Mn_{0.1}Co_{(0.1-x)}Ti_xO_2$ (a) x = 0.01, (b) x = 0.02, and (c) x = 0.03

CONCLUSION

We have successfully synthesized and characterized cathode materials with Ti^{4+} substitution. SEM findings indicated that the particles experienced agglomeration, with a typical proportion of the primary particles ranging from 300-500 nm and the secondary particle sizes ranging from 1-3 μm. The morphology of the samples showed polycrystals. The maximum electronic conductivity obtained was 2.3 x 10^{-5}, 2.4 x 10^{-5}, and 3.2 x 10^{-5} S/cm, for x = 0.01, 0.02, and 0.03, respectively. Another impact of the substitution of Ti^{4+} is to increase the cell volume and conductivity, and the sample can be used as a battery cathode.

ACKNOWLEDGMENT

This work was supported by Universitas Pelita Harapan Grants 2020 No. P-35-FIP/XII/2021.

AUTHOR CONTRIBUTIONS

Maya Puspitasari Izaak: Supervision, Methodology, and Writing - Review & Editing; Yohanes Edi Gunanto: Investigation, Conceptualization, Validation, and Writing - Original Draft; Henni Sitompul: Formal Analysis and Writing - Review & Editing; Yustinus Purwamargapratala: Investigation and Formal Analysis.

DECLARATION OF COMPETING INTEREST

The authors declare that they have no known competing financial interests or personal relationships that could have appeared to influence the work reported in this paper.

REFERENCES

[1] Ellingsen LAW and Hung CR. *Research for TRAN Committee - Battery-powered electric vehicles: market development and lifecycle emissions study*. Washington DC: European Parliament; 2018.
[2] Sim SJ, Lee SH, Jin BS, and Kim HS. Use of carbon coating on $LiNi_{0.8}Co_{0.1}Mn_{0.1}O_2$ cathode

material for enhanced performances of lithium-ion batteries. *Scientific Reports*. 2020; **10**: 11114. DOI: https://doi.org/10.1038/s41598-020-67818-5.

[3] Li S, et al. Mutual modulation between surface chemistry and bulk microstructure within secondary particles of nickel-rich layered oxides. *Nature Communications*. 2020; **11**: 4433. DOI: https://doi.org/10.1038/s41467-020-18278-y.

[4] Ghatak K, Basu S, Das T, Sharma V, Kumar H, and Datta D. Effect of Cobalt Content on the Electrochemical Properties and Structural Stability of NCA Type Cathode Materials. *Physical Chemistry Chemical Physics*. 2018; **20**: 22805-22817. DOI: https://doi.org/10.1039/C8CP03237H.

[5] Steiner JD. *Understanding and Controlling the Degradation of Nickel-rich Lithium-ion Layered Cathodes*. Thesis. Virginia: Virginia Polytechnic Institute and State University; 2018.

[6] Widiyandari H, Sukmawati AN, Sutanto H, Yudha C, and Purwanto A. Synthesis of $LiNi_{0.8}Mn_{0.1}Co_{0.1}O_2$ cathode material by hydrothermal method for high energy density lithium-ion battery. *Journal of Physics: Conference Series.* 2019; **1153**: 012074. DOI: https://doi.org/10.1088/1742-6596/1153/1/012074.

[7] Min BS, et al. Structural Changes and Thermal Stability of Charged $LiNi_xMn_yCo_zO_2$ Cathode Materials Studied by Combined In Situ Time-Resolved XRD and Mass Spectroscopy. *ACS Applied Materials and Interfaces*. 2014; **6**(24): 22594–22601. DOI: https://doi.org/10.1021/am506712c.

[8] Liu W, et al. Improvement of the high-temperature, high-voltage cycling performance of $LiNi_{0.5}Co_{0.2}Mn_{0.3}O_2$ cathode with TiO_2 coating. *Journal of Alloys and Compound*. 2012; **543**: 181–188. DOI: https://doi.org/10.1016/j.jallcom.2012.07.074.

[9] Xie H, Du K, Hu G, Peng Z, and Cao Y. The Role of Sodium in $LiNi_{0.8}Co_{0.15}Al_{0.05}O_2$ Cathode Material and Its Electrochemical Behaviors. *The Journal of Physical Chemistry C*. 2016; **120**(6): 3235–3241. DOI: https://doi.org/10.1021/acs.jpcc.5b12407.

[10] Croguennec L, Suard E, Willmann P, and Delmas C. Structural and Electrochemical Characterization of the $LiNi_{1-y}Ti_yO_2$ Electrode Materials Obtained by Direct Solid-State Reactions. *Chemistry of Materials.* 2002; **14**(5): 2149–2157. DOI: https://doi.org/10.1021/cm011265v.

[11] Tian C, Lin F, and Doeff MM. Electrochemical Characteristics of Layered Transition Metal Oxide Cathode Materials for Lithium-Ion Batteries: Surface, Bulk Behavior, and Thermal Properties. *Accounts of Chemical Research.* 2018; **51**(1): 89–96. DOI: https://doi.org/10.1021/acs.accounts.7b00520.

[12] Yang G, Abraham C, Ma Y, Myoungseok L, Helfrick E, Dahyun O, and Dongkyu L. Advances in Materials Design for All-Solid-state Batteries: From Bulk to Thin Films. *Applied Sciences.* 2020; **10**(14): 4727. DOI: https://doi.org/10.3390/app10144727.

[13] Markus IM, Lin F, Kam KC, Asta M, and Doeff M M. Computational and Experimental Investigation of Ti Substitution in $Li_1(Ni_xMn_xCo_{1-2x-y}Ti_y)O_2$ for Lithium Ion Batteries. *The Journal of Physical Chemistry Letters*. 2014; **5**(21): 3649-3655. DOI: https://doi.org/10.1021/jz5017526.

[14] Jonderian A and McCalla E. The role of metal substitutions in the development of Li batteries, part II: solid electrolytes. *Materials Advances*, 2021; **2**(9): 2846-2875. DOI: https://doi.org/10.1039/D1MA00082A.

[15] Zheng F, Kotobuki M, Song S, Lai M O, and Lu L. Review on solid electrolytes for all-solid-state lithium-ion batteries. *Journal of Power Sources*. 2018; **389**: 198–213. DOI:

https://doi.org/10.1016/j.jpowsour.2018.04.022.

[16] Sun X, Xu Y, Chen G, Ding P, and Zheng X. Titanium doped LiVPO4F cathode for lithium ion batteries. *Solid State Ionics*. 2014; **268**(B): 236-241. DOI: https://doi.org/10.1016/j.ssi.2014.08.008.

[17] Yao W, Liu Y, Li D, Zhang Q, Zhong S, Cheng H, and Yan Z. Synergistically Enhanced Electrochemical Performance of Ni-rich Cathode Materials for Lithium-ion Batteries by K and Ti Co-modification. *The Journal of Physical Chemistry C*. 2020; **124**(4): 2346-2356. DOI: https://doi.org/10.1021/acs.jpcc.9b10526.

[18] Liang L, Sun X, Zhang J, Hou L, Sun J, Liu Y, Wang S, and Yuan C. In Situ Synthesis of Hierarchical Core Double-Shell Ti-Doped $LiMnPO_4$@$NaTi_2(PO_4)_3$@C/3D Graphene Cathode with High-Rate Capability and Long Cycle Life for Lithium-Ion Batteries. *Advanced Energy Materials*. 2019; **9**(11): 1802847. DOI: https://doi.org/10.1002/aenm.201802847.

[19] Sun H, Cao Z, Wang T, Lin R, Li Y, Liu X, Zhang L, Lin F, Huang Y, and Luo W. Enabling high-rate performance of Ni-rich layered oxide cathode by uniform titanium doping. *Materials Today Energy*. 2019; **13**: 145–151. DOI: https://doi.org/10.1016/j.mtener.2019.05.003.

[20] Wan DY, et al. Effect of Metal (Mn, Ti) Doping on NCA Cathode Materials for Lithium-Ion Batteries. *Journal of Nanomaterials*. 2018; **2018**: 8082502. DOI: https://doi.org/10.1155/2018/8082502.

[21] Liu H, Naylor A J, Menon AS, Brant WR, Edström K, and Younesi R. Understanding the Roles of Tris (trimethylsilyl) Phosphite (TMSPi) in $LiNi_{0.8}Mn_{0.1}Co_{0.1}O_2$ (NMC811)/Silicon–Graphite (Si–Gr) Lithium-Ion Batteries. *Advanced Materials Interfaces*. 2020; **7**(15): 2000277. DOI: https://doi.org/10.1002/admi.202000277.

[22] Savina AA, Orlova ED, Morozov AV, Luchkin SY, and Abakumov AM. Sulfate-Containing Composite Based on Ni-Rich Layered Oxide $LiNi_{0.8}Mn_{0.1}Co_{0.1}O_2$ as High-Performance Cathode Material for Li-ion Batteries. *Nanomaterials*. 2020; **10**(12): 2381. DOI: https://doi.org/10.3390/nano10122381.

[23] Cabelguen PE, Peralta D, Cugnet M, and Maillet P. Impact of Morphological Changes of $LiNi_{1/3}Mn_{1/3}Co_{1/3}O_2$ on Lithium-Ion Cathode Performances. *Journal of Power Sources*. 2017; **346**: 13–23. DOI: https://doi.org/10.1016/j.jpowsour.2017.02.025.

[24] Chen Z, Wang J, Chao D, Baikie T, Bai L, Chen S, Zhao Y, Sum T C, Lin J, and Shen Z. Hierarchical Porous $LiNi_{1/3}Co_{1/3}Mn_{1/3}O_2$ Nano-/Micro Spherical Cathode Material: Minimized Cation Mixing and Improved Li^+ Mobility for Enhanced Electrochemical Performance. *Scientific Reports*. 2016; **6**: 25771. DOI: https://doi.org/10.1038/srep25771.

[25] Teichert P, Eshetu GG, Jahnke H, and Figgemeier E. Degradation and Aging Routes of Ni-Rich Cathode Based Li-Ion Batteries. *Batteries*. 2020; **6**(1): 8. DOI: https://doi.org/10.3390/batteries6010008.

[26] Ju-Myung K, Zhang X, Ji-Guang Z, Manthiram A, Meng Y S, and Wu X. A review on the stability and surface modification of layered transition-metal oxide cathodes. *Materials Today*. 2021; **46**: 155-182. DOI: https://doi.org/10.1016/j.mattod.2020.12.017.

[27] Wan D Y, Fan Z Y, Dong Y X, Baasanjav E, Hang-Bae J, Bo J, Jin E M, and Sang Mun J, Effect of Metal (Mn, Ti) Doping on NCA Cathode Materials for Lithium Ion Batteries. *Journal of Nanomaterials*. 2018; **2018**: 808252. https://doi.org/10.1155/2018/8082502.

[28] Ding YL, Cano ZP, Yu A, Lu J, and Chen Z. Automotive Li-Ion Batteries: Current Status and Future Perspectives. *Electrochemical Energy Reviews*. 2019; **2**: 1–28. DOI: https://doi.org/10.1007/s41918-018-0022-z.

[29] Zhang D, Liu Y, Wu L, Feng L, Jin S, Zhang R, and Jin M. Effect of Ti ion doping on electrochemical performance of Ni-rich $LiNi_{0.8}Co_{0.1}Mn_{0.1}O_2$ cathode material. *Electrochimica Acta*. 2019; **328**: 135086. https://doi.org/10.1016/j.electacta.2019.135086.

[30] Zheng F, Kotobuki M, Song S, Lai M O, and Lu L. Review on solid electrolytes for all-solid-state lithium-ion batteries. *Journal of Power Sources*. 2018; **389**: 198–213. DOI: https://doi.org/10.1016/j.jpowsour.2018.04.022.

[31] Mahey S, Kumar R, Sharma M, Kumar V, and Bhardwaj R. A critical review on toxicity of cobalt and its bioremediation strategies. *SN Applied Science.* 2020; **2**: 1279. DOI: https://doi.org/10.1007/s42452-020-3020-9.

[32] Engwa GA, Ferdinand PU, Nwalo FN, and Unachukwu MN. Mechanism and health effects of heavy metal toxicity in humans. *Poisoning in the modern world-new tricks for an old dog*. 2019; **10**: 70-90. DOI: https://doi.org/10.5772/intechopen.82511.

[33] Fu Z and Xi S. The effects of heavy metals on human metabolism. *Toxicology mechanisms and methods*. 2020; **30**(3): 167-176. DOI: https://doi.org/10.1080/15376516.1701594.

[34] Qadrdan M, Jenkins N, and Wu J. Chapter II-3-D - Smart Grid and Energy Storage. In Kalogirou SA, *McEvoy's Handbook of Photovoltaics (Third Edition)*. Amsterdam: Elsevier; 2018: 915-928. DOI: https://doi.org/10.1016/B978-0-12-809921-6.00025-2.